AIP Applied Physics Letters

The characteristic carrier–Er interaction distance in Er-doped a-Si/SiO2 superlattices formed by ion sputtering

Ji-Hong Jhe, Jung H. Shin, Kyung Joong Kim, and Dae Won Moon

Citation: Appl. Phys. Lett. 82, 4489 (2003); doi: 10.1063/1.1586458
View online: http://dx.doi.org/10.1063/1.1586458
View Table of Contents: http://apl.aip.org/resource/1/APPLAB/v82/i25
Published by the American Institute of Physics.

Additional information on Appl. Phys. Lett.

Journal Homepage: http://apl.aip.org/
Journal Information: http://apl.aip.org/about/about_the_journal
Top downloads: http://apl.aip.org/features/most_downloaded
Information for Authors: http://apl.aip.org/authors

ADVERTISEMENT

Downloaded 18 Apr 2013 to 143.248.118.122. This article is copyrighted as indicated in the abstract. Reuse of AIP content is subject to the terms at: http://apl.aip.org/about/rights_and_permissions

The characteristic carrier–Er interaction distance in Er-doped *a*-Si/SiO_2 superlattices formed by ion sputtering

Ji-Hong Jhe and Jung H. Shin[a)]
Department of Physics, Korea Advanced Institute of Science and Technology (KAIST), 373-1 Kusung-dong, Yusung-gu, Taejon, Korea

Kyung Joong Kim and Dae Won Moon
Nano Surface Group, Korea Research Institute of Standards and Science (KRISS), Taejon 305-606, Korea

(Received 12 September 2002; accepted 22 April 2002)

The characteristic interaction distance between Er^{3+} ions and carriers that excite them in Er-doped *a*-Si/SiO_2 superlattices is investigated. Superlattice thin films consisting of 12 periods of *a*-Si/SiO_2:Er/SiO_2/SiO_2:Er layers were deposited by ion sputtering and subsequent annealing at 950 °C. The dependence of the Er^{3+} photoluminescence intensity on the thickness of the Er-doped SiO_2 layers is well-described by an exponentially decreasing Er-carrier interaction with a characteristic interaction distance of 0.5 ± 0.1 nm. © *2003 American Institute of Physics.*
[DOI: 10.1063/1.1586458]

Er^{3+} luminesces at 1.54 μm due to the intra-4*f* transition from the first excited to the ground state ($^4I_{13/2}\rightarrow{}^4I_{15/2}$), coincident with the absorption minimum of silica-based optical fibers. As this transition is parity-forbidden, and occurs only due to the parity-breaking effects of the crystal field, the luminescence lifetime tends to be very long (>ms). This allows for easy population inversion, and has allowed development erbium-doped fiber amplifiers that enabled the realization of all optical telecommunication networks.[1]

Yet, for the same reason, the optical absorption cross-section of Er^{3+} is very small, necessitating the use of expensive lasers for excitation. However, if Er^{3+} is doped into Si, then it can be excited via an Auger-type interaction with photogenerated excitons in Si.[2–5] Since only carrier generation is necessary, and since the absorption cross section of Si is several orders of magnitude greater than that of Er^{3+}, this carrier-mediated excitation allows, in principle, the use of low-cost, broadband light sources such as light-emitting diodes for efficient excitation of Er^{3+}. However, despite some early successes, the room-temperature Er^{3+} luminescence efficiencies from Er-doped bulk Si remain too low to be practical.[4,5]

However, it has been demonstrated that by using either Si nanoclusters embedded inside an SiO_2 matrix[6–8] or Si/SiO_2 superlattice (SL) with nanometer-thick Si layers[9,10] as the host material, it is possible to obtain both the high excitation efficiency of Si and the high luminescence efficiency of SiO_2. In such cases, Er^{3+} luminescence is dominated by Er^{3+} ions located outside, but close to, Si clusters.[11–13] Thus, Si clusters act as classical sensitizers, absorbing the pump photons and transferring the energy to Er^{3+}.[14,15] As both optical gain[16] and electroluminescence[17] are possible in such Si nanocluster sensitized Er^{3+}, it may open the way for a compact, active, all-silicon integrated optical devices.

However, a detailed description of the carrier–Er interaction including the characteristic interaction distance is still lacking. Such a description is necessary, not only for designing the optimum material structure for device applications, but also for understanding the physical mechanisms underlying the Er^{3+}–carrier interaction that is not yet fully understood. In this letter, we report on the Er^{3+} luminescence properties of Er-doped *a*-Si/SiO_2 SL films whose Er-doped SiO_2 layer thickness was controlled with subnanometer resolution. We find that experimental data can be well-described by an Er–carrier interaction that decreases exponentially, with a characteristic carrier–Er^{3+} interaction distance of 0.5 ± 0.1 nm, indicating the likelihood of an exchange interaction between carriers and Er^{3+} ions.

Er-doped *a*-Si/SiO_2 superlattices were deposited on Si substrates using the two-target-alternation UHV-ion-beam sputtering method. One sputtering target was a 6-in.-diameter *p*-type Si wafer, and the other was a similar Si wafer with an Er metal piece (99.9% purity) centered on the wafer. The base pressure of the system is less than 1×10^{-8} Torr, and a 570-eV Ar^+ beam from an ion gun was used to sputter the targets. The Si layers were deposited by sputtering using the Ar^+ beam only, and the SiO_2 layers were deposited by sputtering in an oxygen pressure of 4.5×10^{-4} Torr. The samples were deposited at room temperature. The deposited films consisted of 12 periods of *a*-Si/SiO_2:Er/SiO_2/SiO_2:Er layers. The thicknesses of the *a*-Si layers were fixed at 1.2 nm. The thicknesses of the SiO_2:Er (Er-doped SiO_2) and SiO_2 (pure SiO_2) layers was varied such that the SiO_2:Er layer thickness increased from 0 to 4.1 nm, while the SiO_2 layer thickness decreased accordingly to keep the thickness of the total SiO_2 layer fixed at 9.5 nm. Such preparation is necessary to ensure that the overall film structure is the same for all films, and that the results will not be affected by optical artifacts caused by multiple reflections. Finally, a 5-nm-thick Si cap layer was deposited on the top. Two sets of samples, one with an Er concentration of 0.27 at. % and the other with 0.1 at. %, were prepared. After deposition, all films were rapid thermal annealed in a sequence of 20 min at 600 °C, 5 min at 950 °C, and 5 min at 600 °C in a flowing N_2 atmosphere to avoid cracking and spalling of the films.

[a)]Electronic mail: jhs@mail.kaist.ac.kr

0003-6951/2003/82(25)/4489/3/$20.00 © 2003 American Institute of Physics

Downloaded 18 Apr 2013 to 143.248.118.122. This article is copyrighted as indicated in the abstract. Reuse of AIP content is subject to the terms at: http://apl.aip.org/about/rights_and_permissions

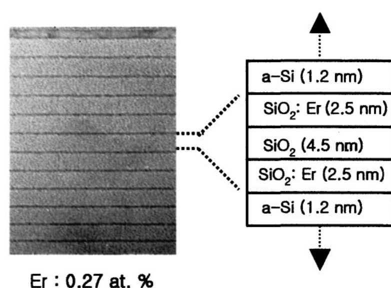

FIG. 1. Bright-field cross-section TEM image of the SL with Er-doped SiO_2 layer thickness of 2.5 nm after annealing. The thin, dark bands are a-Si layers and gray bands are SiO_2 layers. On the right is a schematic drawing showing the composition of the layers.

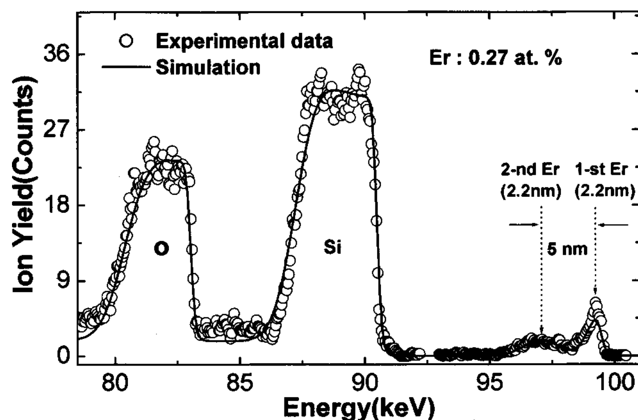

FIG. 2. MEIS spectrum for the SiO_2:Er/SiO_2/SiO_2:Er layers with thicknesses of 2.2, 5, and 2.2 nm, respectively. The symbols are experimental data and the line is the result of simulation.

The Er^{3+} photoluminescence (PL) spectra were taken at room temperature using a grating monochromator, a thermoelectrically cooled InGaAs detector, and the standard lock-in technique. The 477-nm line of an Ar laser, which is not absorbed optically by Er^{3+}, was used as the excitation source to ensure that excitation of Er^{3+} occurs via carriers only. The excitation power was kept at 100 mW to remain in the weak pumping regime, as it was determined that Er^{3+} PL intensity increased linearly with the pump power up to 150 mW (not shown). Time-resolved Er^{3+} luminescence was measured using a digitizing oscilloscope. The structure and composition of the films were analyzed using transmission electron microscopy (TEM) and medium-energy ion scattering spectroscopy (MEIS). The MEIS analyses were done using a 100-keV H^+ beam aligned to the [001] direction in the (011) plane. H^+ ions scattered into the [111] direction were analyzed at a scattering angle of 125°. For MEIS analysis, a sample consisting of a single period of SiO_2:Er/SiO_2/SiO_2:Er layers with intended thicknesses of 2.2, 5, and 2.2 nm, respectively, was deposited and annealed under identical conditions.

Figure 1 shows the bright-field cross-section TEM image of a deposited and annealed SL film with 0.27 at. % Er and the schematic depiction of its intended structure. The dark and gray bands correspond to the Si and SiO_2 layers, respectively. We find that the Si and the SiO_2 layer thicknesses are 1.2 and 9.5 nm, respectively, in good agreement with the intended thicknesses. Note that the Si layers are amorphous despite the high-temperature annealing that crystallized the cap layer. This is consistent with reports by other researchers that nanometer-thick Si layers are very difficult to crystallize.[18,19]

The MEIS spectrum is shown in Fig. 2. The symbols are the experimental data, and the line is the result of the simulation. We find that thicknesses of SiO_2:Er/SiO_2/SiO_2 layers are 2.2, 5, and 2.2 nm, in an excellent agreement with the intended thicknesses. The Er concentration was 0.27 at. % for both SiO_2:Er layers. Taken together, Figs. 1 and 2 confirm that we can deposit a-Si/SiO_2:Er/SiO_2/SiO_2:Er layers with subnanometer control over the individual layers, while keeping the overall film structure the same.

Figure 3 shows the dependence of the Er^{3+} peak PL intensity from the sample with 0.27 at. % Er on the SiO_2:Er layer thickness. The inset shows that from the sample with 0.1 at. % Er. The symbols are the experimental data, and the lines are the results of the fit discussed later. We find that for both sets of samples, the Er^{3+} PL intensity increases with increasing SiO_2:Er layer thickness d, but saturates quickly after only about 1.5 nm, and remains constant thereafter.

Figure 4 shows the dependence of the Er^{3+} luminescence lifetimes on the SiO_2:Er layer thickness from the films with 0.27 at. % Er. We find that the Er^{3+} luminescence lifetime is independent of the SiO_2:Er layer thickness d, being about 0.6 ms for all films. A similar quantitative analysis on the films with 0.1 at. % Er was not possible due to the low Er^{3+} PL intensity. However, they, too, did not display any strong dependence of the Er^{3+} luminescence lifetimes on the SiO_2:Er layer thickness (data not shown).

Changes in the Er^{3+} PL luminescence intensity can occur due to changes in the excitation rate, the Er^{3+} luminescence efficiency, and the number of available Er^{3+} ions. In the present case, since the overall film structure is the same for all films, the generation rate of carriers that can excite Er^{3+} ions should be the same for all films. Furthermore, as Fig. 4 shows, the Er^{3+} luminescence efficiency is the same for all films as well. Thus, the increase in the Er^{3+} PL intensity with increasing SiO_2:Er layer thickness indicates that

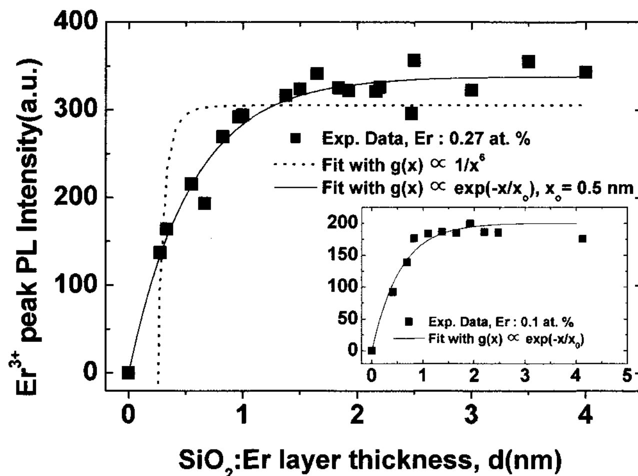

FIG. 3. The dependence of the Er^{3+} peak PL intensities on the SiO_2:Er layer thickness in Er-doped a-Si/SiO_2 SLs. The symbols are experimental data and the lines are the results of fits using different carrier–Er^{3+} interaction mechanisms. The inset shows the dependence of the Er^{3+} peak PL intensities on the SiO_2:Er layer thickness in Er-doped a-Si/SiO_2 SLs containing 0.1 at % Er and the line is the result of fit.

Downloaded 18 Apr 2013 to 143.248.118.122. This article is copyrighted as indicated in the abstract. Reuse of AIP content is subject to the terms at: http://apl.aip.org/about/rights_and_permissions

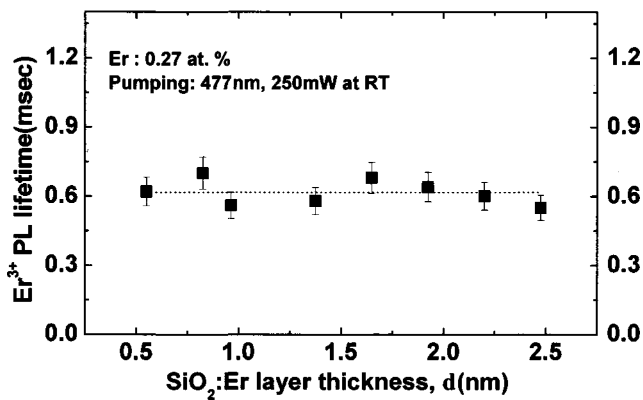

FIG. 4. The dependence of the Er^{3+} luminescence lifetimes on the SiO_2:Er layer thickness in Er-doped a-Si/SiO_2 SLs containing 0.27 at % Er. The dotted line represents the average lifetime.

the number of available Er^{3+} ions is increasing, that is, excitation of Er^{3+} can occur over atomic distances and is not limited to a-Si/SiO_2:Er interfaces.

In such a case, we can write the excitation dynamics of Er^{3+} as

$$\frac{dN^*(x)}{dt} = g(x)(N_o - N^*) - \frac{N^*(x)}{\tau}, \tag{1}$$

where x is the distance from the a-Si layer, $N^*(x)$ is the number of excited Er^{3+} at x, $g(x)$ is the distance-dependent carrier-mediated excitation rate, N_o is the number of excitable Er^{3+} ions at x (fixed by the Er concentration), and τ is the decay rate of excited Er^{3+} ions that include all possible nonradiative decay mechanisms. In steady state, $dN^*/dt = 0$, and $N^*(x) = [g(x)\tau N(x)]/[g(x)\tau + 1]$. However, in the linear, weak pumping regime, $g(x)\tau \ll 1$, and we can accurately approximate:[4,5,20]

$$N^*(x) \cong g(x)\tau N_o. \tag{2}$$

The total Er^{3+} intensity is $\propto \int g(x)\tau N_o$. Clearly, $g(x)$ has to decrease with distance, and the monotonic increase of the Er^{3+} PL intensity to a saturation value indicates that $g(x)$ decreases monotonically with distance. The two well-known interaction mechanisms involving carriers and emission centers such as Er^{3+} with such characteristics are resonant dipole–dipole interaction and the exchange interaction.[21] In the former, the interactions decreases as x^{-6}, while in the latter, the interaction decreases as $\exp(-x/x_o)$.[22] Thus, Eq. (2) was integrated using both forms for $g(x)$, and fitted to the data shown in Fig. 3. We find that the exponential form for $g(x)$ with a value of 0.5 ± 0.1 nm for x_o describes the data much better than the polynomial form. In fact, increasing the power of x to take into account the possibility of multipole interaction did not result in any improvement of the fit (not shown). We note that, as is shown in the inset, the result for the sample with 0.1 at. % Er can also be described very well with an exponentially decreasing interaction with the same x_o, further confirming the validity of the fit.

The value of 0.5 ± 0.1 nm is quite small, indicating that the SiO_2:Er layers in an a-Si/SiO_2:Er/a-Si SL must be kept very thin—less than 2 nm—for maximum efficiency. Furthermore, the exponentially decreasing interaction indicates that an exchange interaction between carries generated in a-Si and Er^{3+} ions in the SiO_2 is much more likely to be dominant than the direct, resonant dipole–dipole interaction between them. We note that Kimura *et al.*, using pre-oxidized porous Si, have come to a similar conclusion.[23] However, the value of x_o was much larger in his case (2–3 versus 0.5 nm). The reason for such differences is not yet clear at this moment. We note, however, that his film contained crystalline Si rather than amorphous Si. Such differences in the Si layers may significantly impact the carrier–Er^{3+} interaction. Finally, we note that the characteristic carrier–Er^{3+} interaction distance may also be dependent on other parameters, such as the Er concentration and the temperature. More detailed investigations are currently on the way.

In conclusion, we have investigated the carrier–Er^{3+} interaction in a-Si/SiO_2:Er/a-Si superlattice films deposited by ion-beam sputtering. We find that the experimental results are well-described by exponentially decaying carrier–Er interactions with a characteristic interaction distance of 0.5 ± 0.1 nm, indicating the likelihood of an exchange interaction between carriers and Er^{3+}.

This work was supported in part by Advanced Photonics Project, the NRL project, and ASSRC at Yonsei University.

[1] *Condensed Matter and Materials Physics* (National Research Council, National Academic Press, Washington, D.C., 1999).
[2] H. Ennen, J. Schneider, G. Pomrenke, and A. Axmann, Appl. Phys. Lett. **43**, 943 (1983).
[3] I. N. Yassievich and L. C. Kimerling, Semicond. Sci. Technol. **8**, 718 (1993).
[4] J. Palm, F. Gan, B. Zheng, J. Michel, and L. C. Kimerling, Phys. Rev. B **54**, 17603 (1996).
[5] F. Priolo, G. Franzò, S. Coffa, and A. Carnera, Phys. Rev. B **57**, 4443 (1998).
[6] A. J. Kenyon, P. F. Trwoga, M. Federighi, and C. W. Pitt, J. Phys.: Condens. Matter **6**, L319 (1994).
[7] M. Fujii, M. Yoshida, Y. Kanzawa, S. Hayashi, and K. Yamamoto, Appl. Phys. Lett. **71**, 1198 (1997).
[8] J. H. Shin, M. J. Kim, S. Y. Seo, and C. C. Lee, Appl. Phys. Lett. **72**, 1092 (1998).
[9] J. H. Shin, W. H. Lee, and H. S. Han, Appl. Phys. Lett. **74**, 1573 (1999).
[10] Y. H. Ha, S. H. Kim, D. W. Moon, J. H. Jhe, and J. H. Shin, Appl. Phys. Lett. **79**, 287 (2001).
[11] M. Stepikhova, W. Jantsch, G. Kocher, L. Palmetshofer, M. Shoisswohl, and H. J. Von Bardeleben, Appl. Phys. Lett. **71**, 2975 (1997).
[12] T. Dejima, R. Saito, S. Yogo, H. Isshiki, and T. Kimura, J. Appl. Phys. **84**, 1036 (1998).
[13] J. H. Shin, J. H. Jhe, S. Y. Seo, Y. H. Ha, and D. W. Moon, Appl. Phys. Lett. **76**, 3567 (2000).
[14] P. G. Kik, M. L. Brongersma, and A. Polman, Appl. Phys. Lett. **76**, 2325 (2000).
[15] G. Franzò, D. Pacifici, V. Vinciguerra, F. Priolo, and F. lacona, Appl. Phys. Lett. **76**, 2167 (2000).
[16] H. S. Han, S. Y. Seo, J. H. Shin, and N. K. Park, Appl. Phys. Lett. **81**, 3720 (2002).
[17] Y. Chen, G. Z. Ran, L. Dai, B. R. Zhang, G. G. Qin, Z. C. Ma, and W. H. Zong, Appl. Phys. Lett. **80**, 2496 (2002).
[18] L. Tsybeskov, K. D. Hirschman, S. P. Duttagupta, M. Zacharias, P. M. Fauchet, J. P. McCaffrey, and D. J. Lockwood, Appl. Phys. Lett. **72**, 43 (1998).
[19] M. Zacharias, J. Bläsing, and P. Veit, L. Tsybeskov, K. D. Hirschman, P. M. Fauchet, J. P. McCaffrey, and D. J. Lockwood, Appl. Phys. Lett. **74**, 2614 (1999).
[20] P. G. Kik, M. J. A. de Dood, K. Kikoin, and A. Polman, Appl. Phys. Lett. **70**, 1721 (1997).
[21] E. Snoeks, P. G. Kik, and A. Polman, Opt. Mater. (Amsterdam, Neth.) **5**, 159 (1996).
[22] A. Suchocki and J. M. Langer, Phys. Rev. B **39**, 7905 (1989).
[23] T. Kimura, H. Isshiki, S. Ide, T. Shimizu, and T. Ishida, J. Appl. Phys. **93**, 2595 (2003).

Downloaded 18 Apr 2013 to 143.248.118.122. This article is copyrighted as indicated in the abstract. Reuse of AIP content is subject to the terms at: http://apl.aip.org/about/rights_and_permissions